

INVERSE FEL HIGH ENERGY GAIN ACCELERATION SCHEMES OPTIMIZED FOR DIFFERENT ELECTRON BEAM ENERGY RANGES

A.A. Varfolomeev[#], S.V. Tolmachev, A. Varfolomeev Jr., T.V. Yarovoii
RRC “Kurchatov Institute”, Moscow 123182, Russia

Abstract

Vacuum laser acceleration schemes IFEL are investigated in diffraction dominated version. CO₂ laser of TW power is regarded as the IFEL driver.

INTRODUCTION

Up to present time many proof-of-principle experiments on laser acceleration were made and time of laser accelerator models construction is coming. In this report we discuss mainly the pure vacuum acceleration paying more attention to the physics than to technology. Further physics study is necessary since common opinion is not yet elaborated which type of the laser or the plasma acceleration schemes can really be the most efficient in providing high acceleration rates of high brightness particle beams. Our review consists of three parts which include recent experimental data on the vacuum acceleration, projects on developing next stage IFEL experiments in strong laser fields and some new concepts of the vacuum acceleration respectively.

RESULTS ON VACUUM ACCELERATION

We will consider far field acceleration in vacuum and namely Inverse Free Electron Lasers (IFELs). The acceleration process is described by the same as in the FEL physics well known equations. A relatively great total energy gain in the IFEL case makes the whole problem more complicate including the electron beam dynamics evolution, providing stability in the nonlinear interaction processes, the radiation losses as well as some technological aspects as the beam focusing, the undulator tapering for the interaction synchronism providing and etc. First detailed theoretical analyses of this problem for the high energy electrons were given in the papers [1,2]. The IFELs with a focused laser beam demand a more correct approach with using simulations. Interesting experimental results on IFELs have been obtained update [3-8]. All of them are actually proof-of-principles ones.

The achieved acceleration rates (≤ 70 MeV/m) and the total energy gains (≤ 20 MeV) are less impressive than the

acceleration gradients (>100 GeV/m) demonstrated in some Laser-induced Wake Field Accelerators (LWFA) or Plasma Wake Field Accelerators (PWFA). However, this acceleration was demonstrated on small path lengths (~ 1 mm) and the obtained beams had large energy spread (up to 100%) with small number accelerated particles [9].

For increasing acceleration rates the following reserves should be taken into account: laser beam with longer wavelengths is more efficient for the IFELs; laser pulse power can practically be raised up to TW and higher levels (not only by increasing total pulse energy but by shortening the pulse length as well); focused laser beam provides very high fields at the focus which can be used for acceleration. Some of these reserves were used in the work [8] where a record rate (70 MeV/m) has been obtained. All these aspects as well as analysis given below show that the diffraction dominated IFEL scheme is the most perspective for electron acceleration by laser fields up to $1 \div 10$ GeV.

PROTOTYPE OF THE FIRST MODULE OF HIGH RATE IFEL

The original version of the UCLA-Kurchatov Institute project [10,11] can be regarded as a prototype of diffraction dominated IFEL. Schematic layout of the IFEL performance is shown in Fig. 1. The 14 MeV electron beam from a photoinjector+booster linac system enter the undulator. A CO₂ laser beam in Gaussian mode is focused by a lens with focal distance of 2.6 m to a tight spot of a few hundreds microns. Basic parameters of the IFEL device are given in Table 1. Very specific undulator construction was constructed with strong tapering and small magnetic field tolerances [12]. Both the magnetic fields and the undulator periods have been tapered to provide synchronism of the laser beam interaction with a captured electron bunch along the entire undulator length. Non-adiabatic approach and numerical 3D simulations were made. Fig. 2 shows the undulator magnetic field profiles and simulated electron energies. Characteristics of the output electron beam are presented in Table 2.

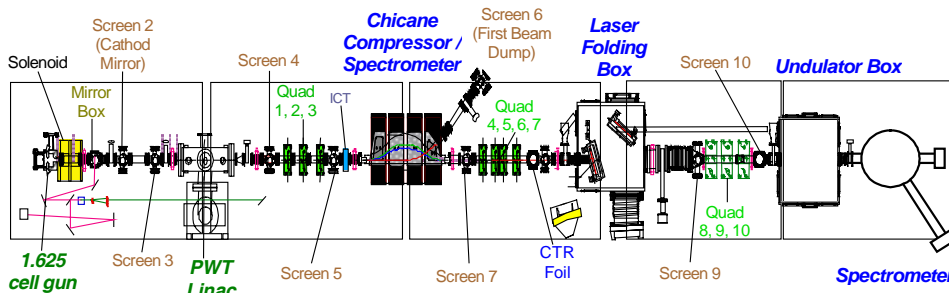


Figure 1. Schematic layout of the IFEL device for the experiment.

Table 1: Basic parameters of the IFEL device.

Laser beam parameters:	
Wave length λ	10.6 μm
Power range	0.4 – 0.8 TW
Pulse length	240 ps
Rayleigh length z_R	3.6 cm
Waist at the focus w_0	0.35 mm
Initial electron beam parameters:	
Initial energy	14 MeV
Energy spread	0.5%
Emittance ϵ_n	10 mm \times mrad
Charge	300 pC
Pulse length	6 ps – 3 ps
Rms radius at the focus	0.15 mm
Undulator parameters:	
Total undulator length	524.5 mm
Undulator period at the entrance $\lambda_w(0)$	15.16 mm
Undulator period at the exit $\lambda_w(z_{\text{max}})$	52.1 mm
Initial field strength	0.115 T
Field strength at the exit	0.626 T
Number of periods	17.5

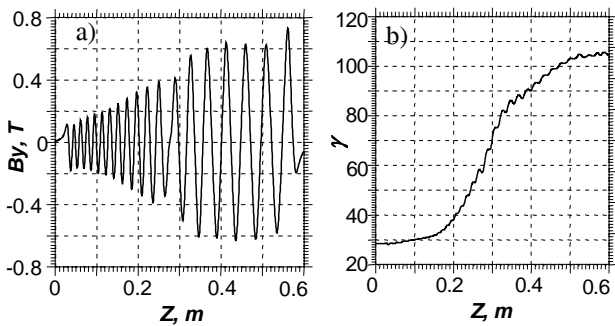


Figure 2: Magnetic fields (a) and accelerated electron energy along the undulator depth (b).

Table 2: Output electron beam parameters from the IFEL.

Energy	55 MeV
Microbunch length	3 fs
Peak current	3 kA
Transverse emittance	10 mm \times mrad
Trapped fraction	>20%

Very important issues: the predicted gain of the accelerated particles is twice larger than in the experiment [8]; b) large accelerating gradient is possible (up to ~ 100 MeV/m); c) appreciable fraction of the primary microbunches is captured for the laser acceleration (tens %).

THE SECOND STAGE OF HIGH RATE IFEL

The second stage Project means design and construction of an additional IFEL module for further acceleration of electron beam after exit from the first IFEL module (Fig. 3). This cascade of two diffraction dominated IFEL modules driven by the same CO₂ high power laser should

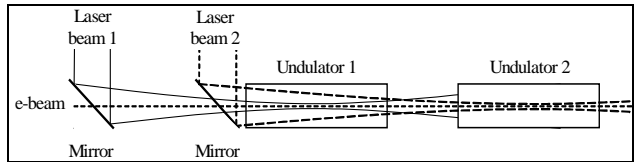


Figure 3: Principal scheme of the two IFEL beam lines.

provide total electron beam acceleration up to 85 MeV [13].

Simulations were made simultaneously for both IFEL acceleration sections so electron beam parameters obtained by simulations at the exit of the first section were used as primary beam parameters for the second IFEL section. Short intersection gap was assumed to be a drift space. The undulator parameters are given in Table 3 and magnetic field profiles are shown in Fig. 4. Simulation results are given in Fig. 5.

Table 3: Parameters of the second IFEL stage undulator.

Period range	4.2 – 5.4 cm
Gap	1.2 cm
Field amplitude range	0.76 – 0.86 T
Total length	63.2 cm
Number of periods	13

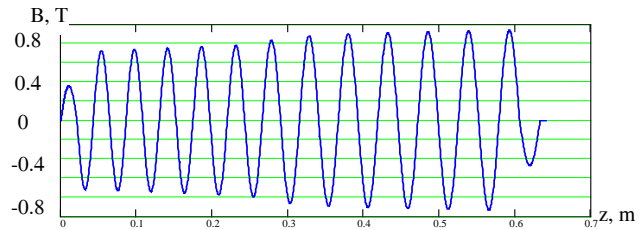


Figure 4: Magnetic field profile along the second IFEL undulator axis.

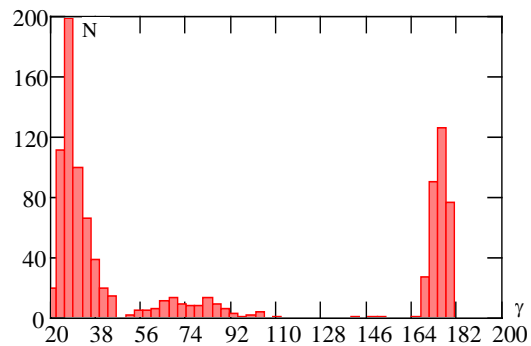


Figure 5: Energy distribution of electrons at the exit of the second IFEL undulator section.

Up to 95% of electrons entering the second undulator can be captured for acceleration and accelerated up to 90 MeV, total capture ratio of the initial beam is 31%.

FREE SPACE ACCELERATION BY GAUSSIAN MODE LASER FIELD

Principal scheme of the free space accelerator is given by Fig. 6. No undulator is using and the laser beam and the electron beam are not collinear. Two mirrors inserted

into resonator turn the Gaussian beam and terminate the laser field interaction with electrons. Small holes in the

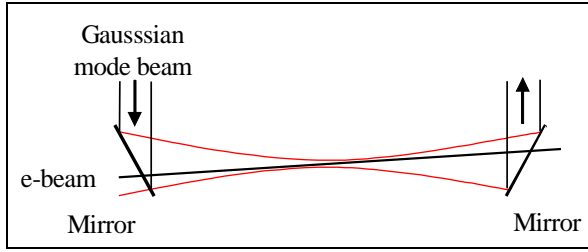


Figure 6: Schematic of the noncollinear interaction with Gaussian mode CO₂ laser beam.

mirrors made for the electron beam propagation are not harmful for the Gaussian mode especially if these holes are out of the first Fresnel zone.

The interaction is proportional to the electric field projection component on the electron beam trajectory E_α , where α is the noncollinearity angle the Guoy phase shift increase the electron slippage. Some compensation of the phase slippage follows from the term noncollinearity [15]. At some α_{opt} slippage variation over z near laser focus becomes more smooth.

The accelerating field profiles of the Gaussian mode are given in Fig. 7. For $\gamma > 600$ the energy exchange is positive in a wide region of the electron beam trajectory and namely in the ranges $-6z_R - +6z_R$. The profiles are practically not dependent on the laser power P and on γ as well (since the used angle α_{opt} does not depend on γ).

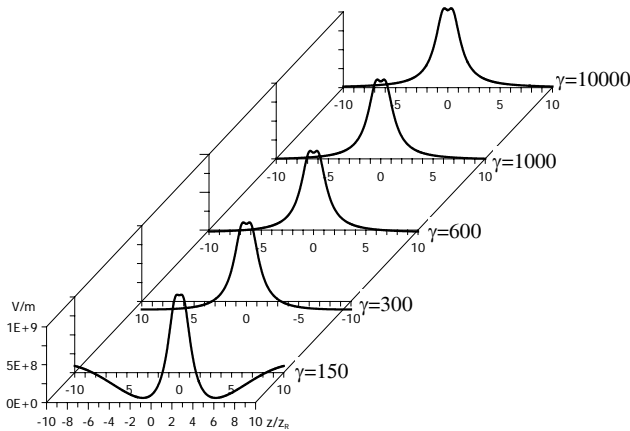


Figure 7: Accelerating field profiles E_α for $z_R=3$ cm, $\alpha = 1/2\sqrt{\lambda_s/2z_R}$, $\Phi_0=\pi/2$, $\lambda=10.6$ μ m, $P=10^{13}$ W.

The acceleration gradients not dependent on the electron energy are given by dE_{el}/dz (MeV/m) = $9.2[\sqrt{P(W)}/z_R$ (m)], where $P(W)$ is the laser power in W.

One of the important problem concerning realization of this free space laser acceleration is focusing of the accelerated beam with conservation of a high precision alignment of the electron beam. Fortunately for the beams

with not small γ the transverse field in the xz plane acting on an electron propagating along the noncollinear trajectory is $F_{tr} = eE_x (1 - \alpha^2\gamma^2)/2\gamma^2$. It is seen that this field provides selffocusing of the electron to the trajectory defined by the slope angle $\alpha = 1/\gamma$. Dynamical phase stability required for the acceleration in the multistage system can be provided as well see for details [15].

CONCLUSION

Short pulses of Gaussian CO₂ laser beam of high power (0.5 – 1.0 TW) can provide 100 – 1000 MeV/m acceleration rate in wide energy range of electrons.

REFERENCES

- [1]. E.D. Courant, C. Pellegrini, W. Zakowicz, Phys. Rev. A32, №5, 2813-2823 (1985)
- [2]. A.A. Varfolomeev, Yu.Yu. Lachin. Sov. Phys. Tech. Phys. 31, No 11, 1273-1278 (1986)
- [3]. I. Wernick, T.C. Marshall, Phys. Rev. A 46, 3566-3568 (1992)
- [4]. A. Van Steenberg, J. Gallardo, et. al., Phys. Rev. Let. 77, 2690-2693 (1996)
- [5]. Y. Liu, X.-J. Wang, D.B. Cline, et. al., Phys. Rev. Let. 80, 4418-4421 (1998).
- [6]. W.D. Kimura, L.P. Campbell, C.E. Dille, et. al., Phys. Rev. Spec. Top. AB 4, 101301-1-101301-12 (2001); Phys. Rev. Lett. 86, 4041 (2001).
- [7]. L.P. Campbell, C.E. Dille, S.C. Gottshalk, et. al. Proceedings of the PAC2003, p.p. 1909-1911.
- [8]. P. Musumeci, S. Tochitsky, S. Boucher, et. al. Proc. of the 26-th Int. FEL Conf., Aug. 29 – Sept. 3, 2004, Trieste, Italy.
- [9]. P. Sprangle, Ch. Joshi, Final Report on the Advanced Acceleration Technique, Proceedings of Snowmass 2001, Working Group, T8.
- [10]. P. Musumeci, C. Pellegrini, et. al., Proceedings of the PAC2001, p.p. 4008-4010.
- [11]. A.A. Varfolomeev, S.V. Tolmachev, et. al., Nucl. Instr. And Meth. A483, 377-382 (2002).
- [12]. S.V. Tolmachev, A.A. Varfolomeev, et. al. Proceedings of the 26-th International Free Electron Laser Conference, Aug. 29 – Sept. 3, 2004, Trieste, Italy.
- [13]. A.A. Varfolomeev, S.V. Tolmachev, et. al. Int. Report CRL-01-04, RRC KI 2004, Moscow.
- [14]. A.A. Varfolomeev, A.H. Hairetdinov, Proceeding of 4 EPAC, p.p. 799-801.
- [15]. A.A. Varfolomeev, A.H. Hairetdinov, AIP Conference Proceedings 279, Ed. J.S. Wurtele, AIP, New York, (1993), p.p. 319-320.
- [16]. A.A. Varfolomeev. Joint Advanced Accelerator and Beam Dynamics Workshop, July 1 – 6, 2002, Chia Laguna, Sardinia, Italy.